Ion acceleration in a gas jet using multi-terawatt CO_2 laser pulses

Chao Gong, Sergei Tochitsky, Jeremy Pigeon, Dan Haberberger, Chan Joshi

Neptune Laboratory, Department of Electrical Engineering, UCLA, Los Angeles, CA, 90095, USA

Abstract. This paper describes ongoing research in the Neptune Laboratory at UCLA on ion acceleration from plasmas formed in different gases using a 4-10TW CO_2 laser. Our experiment is focused on acceleration of Helium and Nitrogen ions using collisionless shocks. The status of the experiment is presented. One dimensional particle-in-cell (PIC) simulations are carried out to study conditions under which a collisionless shock is launched in two interpenetrating plasmas with different charge densities and charge states.

Keywords: laser-driven ion acceleration, CO_2 laser, collisionless shock, 1-D PIC simulation
PACS: 52.38.Kd, 52.35.Tc, 42.55.Ct, 52.65.Rr

INTRODUCTION

Laser-driven ion acceleration (LDIA) is capable of producing accelerated ion beams that can have a short duration, an ultra-low emittance [1], and different charge states [2]. This versatility has caused a lot of interest in the scientific community because of potential application of such ion beams to fast ignition in inertial confinement fusion, ion beam cancer therapy, and also for probing electric field structures in dense plasmas [3].

Here, we report the status of an ongoing research project in the Neptune Laboratory at UCLA on LDIA in plasmas produced in different gases using CO_2 laser pulses. Our current interest is in helium and nitrogen ion acceleration. In this paper we first evaluate using the barrier suppression model, which nitrogen and helium ion states can be expected using a TW class CO_2 laser. Then, we report on the status of the current experiment. Finally, we use 1-D PIC simulation [4] to study the formation of a collisionless shock wave when two plasmas with different charge states interpenetrate into each other.

IONIZATION OF DIFFERENT GASES WITH HIGH POWER CO_2 LASER

Appearance intensity is defined as the intensity at which a small number of ions are produced at a particular charge state [5]. The experimentally obtained values of the appearance intensity are consistent with the barrier suppression model, in which the external static electric field such as that of the laser is superimposed on the Coulomb potential of the atom. At certain intensity the Coulomb barrier is completely suppressed and electrons can escape the atom without the need to tunnel through the barrier. In Fig.1 we plot the various ionization states of helium and nitrogen and their appearance intensities below 8.6×10^{16} W/cm^2, the maximum intensity expected with our laser in vacuum.

The previous successful experiment on proton acceleration [6], carried out in the Neptune Laboratory, used a CO_2 laser pulse produced by a master oscillator power amplifier (MOPA) system [7]. This laser macro-pulse has a temporal envelope with a full width at half maximum (FWHM) of ~100ps. The macro-pulse is modulated periodically as a sequence of 3ps micropulses with 18ps separation due to the splitting of molecular rovibrational lines. In our experiment, the peak normalized vector potential in vacuum deduced for the two largest laser micropulses was typically lager than 1.5 corresponding to a laser intensity higher than 3×10^{16} W/cm^2. As shown in Fig.1, at these CO_2 laser intensities, the nitrogen atoms can be ionized up to N^{5+} while helium atoms can be fully ionized up to He^{2+}.

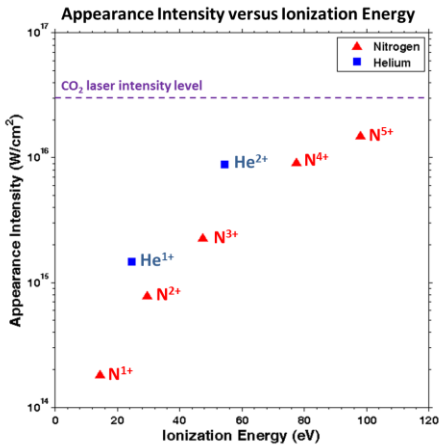

FIGURE 1. Appearance intensity versus ionization energy for nitrogen and helium ions at different charge states

STATUS OF EXPERIMENT

In the past LDIA experiments, the energy delivered into the target chamber was limited by the size of the input window. At present, a new target chamber is installed which can accept a full 5" laser beam with an energy up to 100J.

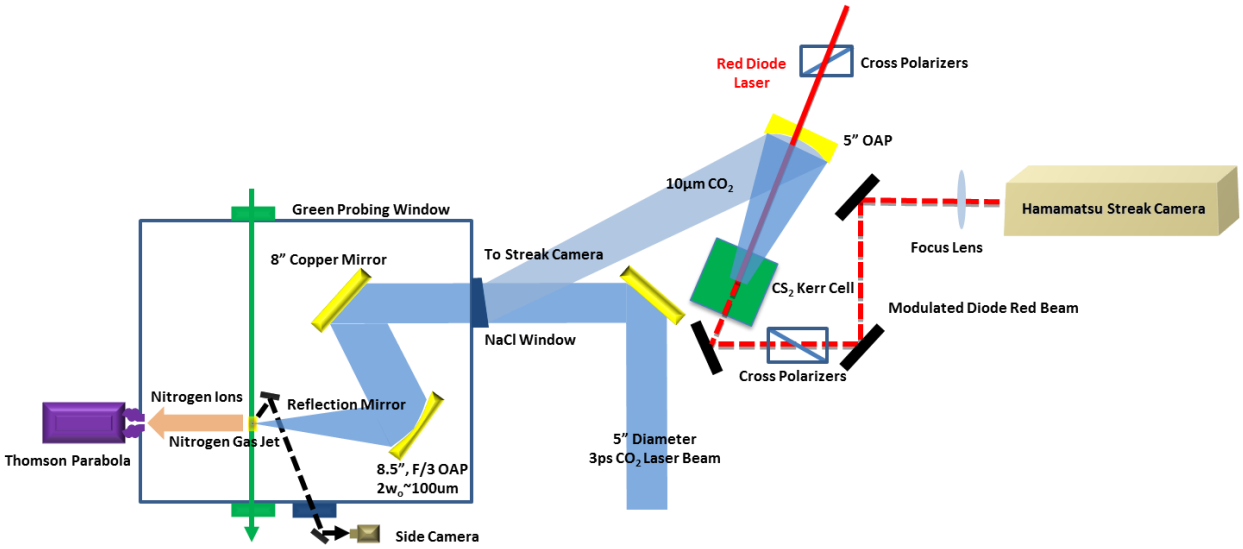

FIGURE 2. Schematic of LDIA experimental setup including a diagnostic for the CO_2 laser pulse length measurement.

As illustrated in Fig. 2, the 5" CO_2 laser beam incident into the target chamber is focused by an 8.5" 60^o off axis parabolic mirror in a gas jet. The side and top cameras (not shown in Fig.2) are installed to position a 1mm gas jet with a precision better than 20μm. To distinguish accelerated nitrogen ions in different ionization states, a Thomson Parabola (TP) ion spectrometer [8] is needed. Using parallel electrical and magnetic fields, TP can deflect particles with a different charge to mass ratio onto non-overlapping parabolic traces and the positions defined on each given trace will determine the particles' energy. In this way, we will be able to study the accelerated nitrogen ions with different charge states and also their energy spectrum. To measure the plasma density profile, a 2ps 532nm probe beam is used for the shadowgraphy in combination with the interferometry diagnostics. A 4% reflection of the CO_2 pulse from the salt window is split from the main beam to gate a red diode laser in a CS_2 Kerr cell. Each pulse's temporal structure is then carried by the red diode beam and measured by a fast streak camera which is sensitive in the visible range only [7].

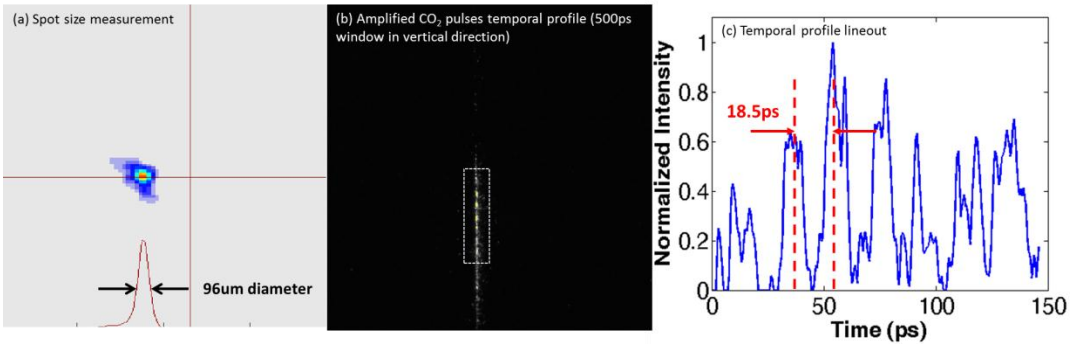

FIGURE 3. (a) CO_2 laser spot size measured in the focus of the OAP. (b), (c) Amplified 10μm CO_2 macro pulse temporal profile.

The focused spot size of an unamplified CO_2 laser beam is measured to be ~100 μm in diameter (FWHM) as shown in Fig.3(a). As expected, the amplified single picosecond pulse evolves into a pulse train with an 18ps pulse separation [7] and the temporal structure is characterized by the Hammamatsu (C5689) streak camera. This temporal profile is shown in Fig.3(b). If we apply the energy partition for a 100J CO_2 laser pulse based on the streak shown in Fig.3(c) and also take into account the measured laser spot size, then the CO_2 laser intensity can be estimated to be $\sim 1.0 \times 10^{17}$ W/cm^2. This intensity is sufficient to ionize nitrogen to N^{5+} and helium to He^{2+} according to the data shown in Fig.1.

ANALYSIS OF SHOCK WAVE ACCELERATION (SWA) IN A PLASMA WITH A MIXTURE OF IONIZATION STATES

Shock wave can be characterized as a disturbance propagating with a velocity faster than sound velocity (c_s). It carries energy and can propagate through various media, including plasma. Normally, shock wave propagation is accompanied with a precipitous change of pressure corresponding to density and/or temperature discontinuity when the medium is plasma. Gauss' law tells us that in the plasma the abrupt change in density associated with a shock implies an abrupt change of propagating electric field. Our previous computer simulations and experiments have shown that a collisionless shock wave due to charge density separation can be launched in a slowly expanding hydrogen plasma by an intense laser pulse. As this shock propagates, it can reflect plasma ions. This can produce a monoenergetic proton beam with an extremely narrow energy spread and very low emittance [6]. Here, we continue our LDIA study to see whether the collisionless shock wave acceleration mechanism can be applied to heavier ions, such as helium and nitrogen. The goal is to understand the conditions under which the shock wave is formed in the plasma with an admixture of different ions and to understand which ions are reflected.

Our previous work has shown that an effective way to generate a collisionless shock is to create an abrupt density change in a very hot plasma [9]. The interpenetration of the higher density plasma (with or without an initial drift velocity) into the lower density plasma is the easiest way to generate such shocks. Here we have extended this finding to the case of heavier ions, using a two semi-infinite plasma slab model. For the case of nitrogen, we simulate and compare the results when N^{5+} plasma expands into either vacuum or into a second N^{2+} plasma. The vacuum expansion simulation allows us to compare how introducing the upstream N^{2+} plasma affects the ambipolar diffusion and how the density ratio of the downstream/upstream plasma affects the shock wave formation. Even though the simulations do not self consistently take into account the effect of the laser pulse in creating such a situation, the downstream N^{5+} plasma can be thought of as that formed by the laser pulse fully ionizing nitrogen atoms up to the 5th ionization state through tunnel ionization near the critical density of a gaseous target. The upstream plasma comprising of N^{2+} ions can be thought of as that produced by electron-neutral collisional ionization by colder plasma electrons produced early during the laser macropulse [6].

Figures 4(a) and 4(b) display snapshots of the charge density lineouts when nitrogen N^{5+} plasma expands into vacuum and when it expands into the N^{2+} plasma for two different initial density ratios of $N^{5+}/N^{2+} = \alpha = 2.5$, and 40. We have also shown the longitudinal electric field for these cases in solid green lines. Initial electron temperature is set at T_e = 550keV for both the upstream and downstream plasmas and the ion temperature is set at 0. At the beginning, the two plasma slabs are separated at the boundary of 995μm in space indicated by a red dash line. And the calculated c_s of N^{2+} is equal to 0.0088c. The red lines in Figures 4(a) and 4(b) show the charge density plots for α

= 2.5 and α = 40. For comparison, the vacuum expansion of the N^{5+} plasma is shown in blue. For lower density ratio α = 2.5, N^{2+} plasma impedes the expansion of the N^{5+} plasma at a high density (n = 0.65× $10^{19}$$cm^{-3}$). This can be observed in Fig.4 (a), where the interpenetration of the upstream plasma into the downstream plasma has propagated up to ~900μm as evidenced by the formation of a nearly constant density plateau over a 100μm thick region. Characteristic rarefaction is observed and measured traveling backward at the sound speed of N^{5+} (c_s = 0.014c). The forward propagating disturbance is measured at a velocity ~0.0068c and thought to be an ion acoustic wave (IAW) launched in the upstream plasma, characterized by bunching of density fluctuation and an oscillatory electric field.

In comparison, higher charge density ratio α = 40 in Fig.4 (b) gives a very different result. The expansion of N^{5+} plasma into the N^{2+} plasma travels much further up to a density of n = 0.25× $10^{19}$$cm^{-3}$ where a shock wave is launched and propagates with a supersonic velocity of 0.0089c in the upstream (c_s = 0.0088c of N^{2+}). The shock is featured with a dominant narrow single spike in the electric field and the ion density as shown in Fig.4 (b).

In the ion phase space, shown in Fig.4 (c) and Fig.4 (d), particle reflection is only observed for the higher charge density ratio case (α = 40), when the shock wave is formed. Both results are carefully compared to the proton cases for the same simulation conditions. It is found that, despite similar values for the longitudinal electric field potentials, due to the heavier ion mass, the amplitude of the IAW and reflected particles momentum for nitrogen ions are smaller than those for protons.

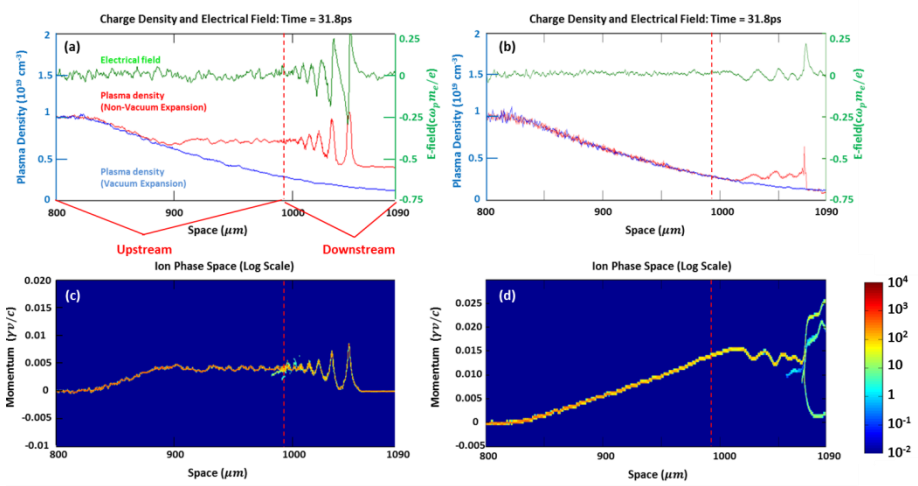

FIGURE 4. Comparisons between N^{5+} plasma expansion into N^{2+} plasma and vacuum. Charge density (red line for plasma expansion and blue line for vacuum expansion) and longitudinal electric field (green line) (a) and ion phase space (c) are plotted at t = 31.8ps. Cases (b) and (d) are the same as above but for α = 40. Color bar shows the population of the simulation particles.

Additionally, half plane simulations also show that introducing an initial relative drift velocity between the two plasma slabs facilitates the shock wave formation. Due to the relative drift velocity, two plasma slabs will penetrate into each other faster thus reducing the required density ratio to launch a shock.

Shock wave formation in the case when N^{5+} plasma streams into N^{2+} plasma for α = 2.5 with different initial relative drift velocities is analyzed in Fig.5. The electron temperature is set as T_e = 511keV and the ion temperature is 0. The color scale is logarithmic to highlight the reflected and trapped simulation particle population. Simulations show that for a small drift velocity, V_{dr} =0.0005c, an IAW is formed and particles start to be trapped in the trailing wave. As V_{dr} increases to 0.005c, upstream ions transmit through the travelling IAW and start to interact with the trailing waves. Through the interaction, the trailing waves are damped and some ions gain enough kinetic energy and bounce off the potential well. Further increment of V_{dr} to 0.02c as in Fig.5(c) shows a significant reflected population of ion bunch with a narrow energy spread. The longitudinal electrical field plot (not shown in the Fig. 5) is characterized with a very narrow single spike which indicates the formation of the shock wave. The shock velocity (V_{sh}) in Fig.5 (c) is measured to be a constant and the velocity of the reflected ions $V_{ions} = 2V_{sh}$.

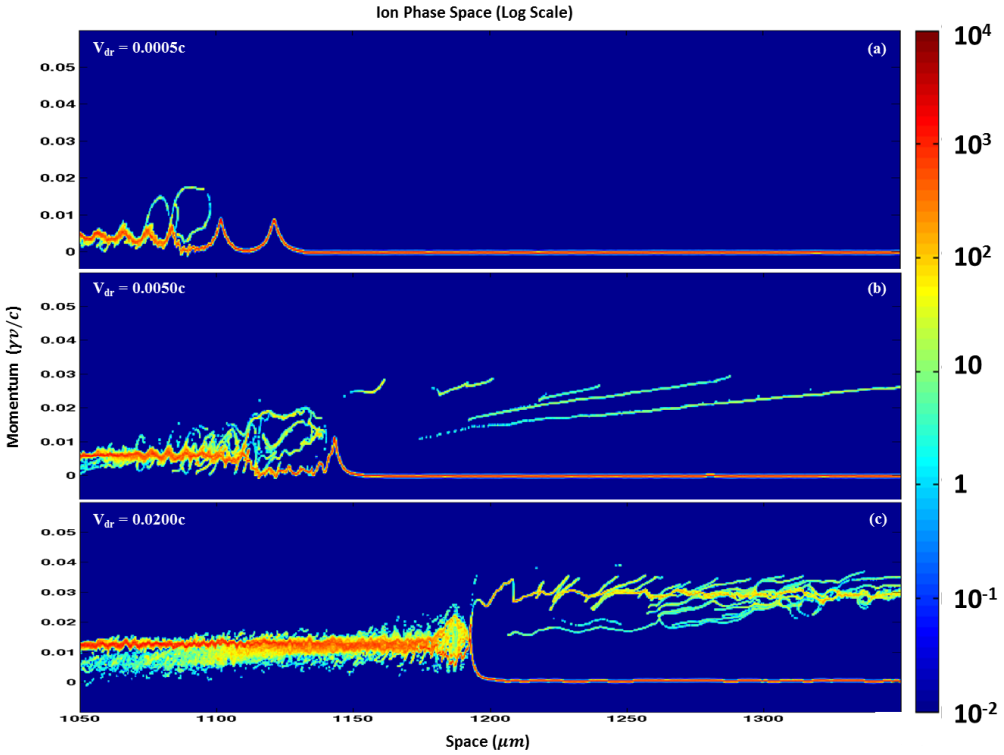

FIGURE 5. Longitudinal ion phase space plotted in the driven case of N^{5+} penetrating into N^{2+}. Time t = 52ps. Density ratio α = 2.5. V_{dr} is equal to (a) 0.0005c, (b) 0.0050c, (c) 0.0200c. Color bar shows the population of the simulation particles.

Last but not the least, the shock formation in the nitrogen ion mixture is simulated by putting N^{5+} in the downstream area and $N^{1+}$and N^{2+} mixture in the upstream area. $N^{1+}$and N^{2+} have the same particle density, and the sum of their density is equal to that of N^{5+}. Temperature gradient is introduced between the two plasma slabs by taking T_e = 1MeV and T_e = 0.5MeV for downstream and upstream electrons, respectively. This allows us to mimic the laser heating condition in the laser-plasma interaction. Ion temperature is set at 0 uniformly across the two plasma slabs. An initial relative drift velocity is introduced at 0.005c, much lower than the hole boring velocity calculated for the downstream N^{5+} ions, which is equal to 0.0216c for a laser intensity ~1×10^{17} W/cm^2 [10]. Simulations show that only N^{2+} ions in the upstream area are reflected by the traveling shock wave. This can be attributed to the fact that N^{1+} ions due to the lower charge state gain less kinetic energy than a minimum required to be reflected off the potential well of the shock wave and thus they simply permeate through. The calculated velocity of the shock wave shown in Fig.6 (b) is equal to 0.0125c which is higher than both of the sound velocity of N^{1+} (0.0063c) and N^{2+} (0.0088c) for the electron temperature T_e = 0.5MeV in the upstream area. The velocity of the reflected N^{2+} ions is ~0.025c, which is close to $2V_{sh}$.

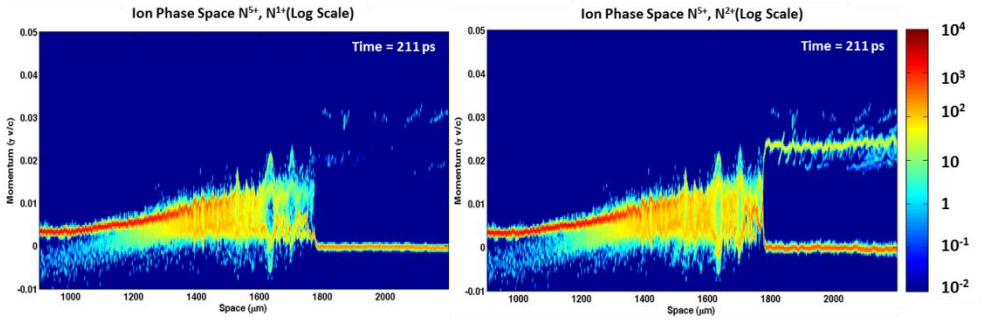

FIGURE 6. Longitudinal ion phase space plotted in the driven case of N^{5+} penetrating into N^{1+} and N^{2+} mixture. V_{dr} = 0.005c. Time t = 211ps. Left figure shows only N^{5+} and N^{1+} in the ion phase space. Right figure shows N^{5+} and N^{2+}.

CONCLUSION

We have presented the status of the ongoing LDIA experiment in the Neptune laboratory of UCLA. 1-D PIC simulations show that SWA mechanism is applicable for the light ion acceleration. For a multiple ion mixture case, when the upstream plasma consists of N^{2+} and N^{1+} ions, simulations show that a shock wave can reflect only N^{2+} ions due to their higher charge state. Future experiments on generation of monoenergetic light ions from CO_2 laser plasma interaction will benefit many applications.

ACKNOWLEDGEMENTS

This work is supported by DOE Grant DE-FG02-92-ER40727, NSF grant PHY-0936266 at UCLA.

REFERENCES

1. Cowan, T.E., et al., *Ultralow emittance, multi-MeV proton beams from a laser virtual-cathode plasma accelerator.* Physical Review Letters, 2004. **92**(20).
2. Hegelich, M., et al., *MeV ion jets from short-pulse-laser interaction with thin foils.* Physical Review Letters, 2002. **89**(8).
3. Ledingham, K.W.D. and W. Galster, *Laser-driven particle and photon beams and some applications.* New Journal of Physics, 2010. **12**.
4. Fonseca, R.A., et al., *OSIRIS: A three-dimensional, fully relativistic particle in cell code for modeling plasma based accelerators.* Computational Science-Iccs 2002, Pt Iii, Proceedings, 2002. **2331**: p. 342-351.
5. Augst, S., et al., *Tunneling Ionization of Noble-Gases in a High-Intensity Laser Field.* Physical Review Letters, 1989. **63**(20): p. 2212-2215.
6. Haberberger, D., et al., *Collisionless shocks in laser-produced plasma generate monoenergetic high-energy proton beams.* Nature Physics, 2012. **8**(1): p. 95-99.
7. Haberberger, D., S. Tochitsky, and C. Joshi, *Fifteen terawatt picosecond CO2 laser system.* Optics Express, 2010. **18**(17): p. 17865-17875.
8. Freeman, C.G., et al., *Calibration of a Thomson parabola ion spectrometer and Fujifilm imaging plate detectors for protons, deuterons, and alpha particles.* Review of Scientific Instruments, 2011. **82**(7).
9. Haberberger, D., et al., aac 2012 proceedings, 2012.
10. Wilks, S.C., et al., *Absorption of Ultra-Intense Laser-Pulses.* Physical Review Letters, 1992. **69**(9): p. 1383-1386.